Catalysis Today 168 (2011) 112–117

Contents lists available at ScienceDirect

Catalysis Today

journal homepage: www.elsevier.com/locate/cattod

Self-assembled titanosilicate TS-1 nanocrystals in hierarchical structures

Louwanda Lakiss, Mickael Rivallan, Jean-Michel Goupil, Jaâfar El Fallah, Svetlana Mintova*

Laboratoire Catalyse & Spectrochimie, ENSICAEN - Université de Caen - CNRS, 6, boulevard du Maréchal Juin, 14050 Caen, France

ARTICLE INFO

Article history:
Received 13 October 2010
Received in revised form
22 December 2010
Accepted 25 December 2010
Available online 4 February 2011

Keywords:
Nanocrystals
Hierarchical structures
TS-1
Porosity
Sorption
Non-thermal plasma

ABSTRACT

Hierarchical structures consisting of microporous titanosilicate TS-1 nanocrystals (MFI-type structure) are obtained by controlled evaporation of colloidal suspensions. The TS-1 nanocrystals with diameter of 60–80 nm are prepared by hydrothermal treatment of clear precursor suspension. The purified TS-1 colloidal suspensions are dried under controlled conditions in order to form hierarchical structures with uniform micropores originated from the TS-1 nanocrystals, mesopores coming from the interparticles spacing and macropores emerging from the controlled evaporation of the solvent. The as-prepared micro/meso/macroporous TS-1 materials are treated by non-thermal plasma to remove the organic template and subsequently characterized by spectroscopy (DLS, IR, UV–vis), microscopy (TEM, SEM), X-ray diffraction, nitrogen sorption and mercury intrusion porosimetry. Besides, the sorption and confinement of 2,4,6-trimethylpyridine (collidine) probe molecule in the micro/meso/macroporous TS-1 structure is followed by FTIR.

1. Introduction

The utilisation of porous materials in catalysis, separation, biochemistry, optics, electronics, electrochemistry, sensors, etc. stimulates the research and focuses more on fabrication of highly porous organized structures featuring multimodal porosity [1–8]. The presence of single micropores in the sorbents or catalysts would result in an undesirable slow diffusion of reactants and products to and from their active sites. The mesoporous materials type MCMs characterized by a high specific surface area and a large tailored pore size are still far from the desired hydrothermal stability and strong acidity as zeolite materials. As a consequence, much research is focused on the development of strategies for preparation of materials with multimodal porosity.

The application of nanosized molecular sieves as building blocks for hierarchical structures is based on the combination of their microporosity and textural porosity, which make them very promising for novel applications especially in catalysis and separation [1,2]. During the last several years, not only the control of the zeolite pore structure and their intra-porous chemistry, but also their external morphology and textural porosity have been largely investigated. Hierarchical structures combining micro/mesopores, micro/macropores, meso/macropores and micro/meso/macropores are usually prepared by using co-surfactant method or dual templated processes [9–11]. In this case, the control of the bimodal porosity is achieved by combining templates with appropriate dimensions and chemical nature, which are supposed to dictate the pore dimensions and features. For example, tetraalkylammonium ions are used for creating the micropores (<2 nm), long chain surfactants or block copolymer micelles for introducing mesopores (2–50 nm), and macro templates such as polystyrene spheres, inorganic fibres, polymers, organized bacterial threads for formation of macropores (>50 nm) [12–14].

Many different approaches have been reported in the literature for creation of hierarchical structures, but the periodicity of the macropores obtained by these methods is still limited and the crystallinity of nanosized building units seem to be not very high. Besides, the fabrication of hierarchical structures using polydimethylsiloxane (PDMS) stamps process, layer by layer technique (LbL) based on alternate deposition of microporous nanoparticles with opposite charges are reported [15,16]. Nanosized zeolite particles have also been infiltrated into the voids of encapsulates by several strategies such as vapour phase transport (VPT), hydrothermal treatments and secondary growth to form structures with variable porosities [17–19]. Most of the reports are based on the use of nanosized zeolite particles as building blocks for creation of hollow spheres, hollow fibres, sponges and foams [17–23] via complex techniques. However, only a few reports on the auto-assembly of these building blocks by a spontaneous reaction such as sedimentation in a gravitational field or attractive capillary forces caused by solvent evaporation are published [13,24,25].

An effort has been focused on the preparation of hierarchical TS-1 material to enhance its catalytic activity in heterogeneous oxidation reactions [26–32]. The high coordination ability of Ti

* Corresponding author. Tel.: +33 231452737; fax: +33 231452822.
E-mail address: svetlana.mintova@ensicaen.fr (S. Mintova).

0920-5861/$ – see front matter © 2011 Elsevier B.V. All rights reserved.
doi:10.1016/j.cattod.2010.12.045

sites associated to the random Si/Ti substitution in the framework results in notable activity for chemical reactions such as aromatic hydroxylation, ammoximation of cyclohexanone to the oxime, olefin epoxidation and alkane oxidation [28–37]. Recently, a number of reports dealing with the preparation of hierarchical features using new synthesis strategies such as introduction of templates or post-synthesis treatment have been published. Preparation and catalytic activity studies on hierarchical TS-1 structures are reported firstly by Jacobsen's group [38]. Beside, the preparation of hierarchical TS-1 in the presence of porogen agents [39,40] and amphiphilic organosilanes [41], and by organofunctionalization of zeolitic seeds followed by crystallization [42] is reported.

In the present work, the preparation of hierarchical TS-1 structure by self-assembly method under controlled water evaporation of colloidal suspensions containing the nanosized TS-1 crystals is reported. A similar approach for fibrous titanium silicalite-1 by drying and evaporation process with lower mechanical stability has been already reported [24].

The TS-1 material is commonly activated through calcination at relatively high temperature leading to the total removing of the organic template from the cavities of the porous material via Hoffman reactions. Such thermal treatment requests slow temperature ramp in order to maintain the high crystallinity of the as-synthesized nanosized crystals and to prevent the nanoparticles from agglomeration leading to change in their porosity. On the other hand, the removal of the structure directing agent (SDA) could be performed via liquid extraction (in acidic or alcohol solutions), microwave-assisted or ozone treatments [43]. Recently, a new route for activation of microporous nanosized BEA-type material by glow discharge process has been described [44]. In this case, the electron and radicals formed in the electrical discharge efficiently lead to removal of the SDA from the micropores at nearly room temperature (RT). In the present case, the TS-1 material has been treated by air plasma at low pressure (5 hPa), and the sorption and confinement of bulky probe molecule (collidine) on the hierarchical TS-1 have been followed by FTIR.

2. Experimental

2.1. Nanosized TS-1 assembled in hierarchical structures

The titanosilicate TS-1 is prepared from clear precursor suspension (molar composition: 9 TPAOH:25 SiO_2:0.14 TiO_2:404 H_2O) under hydrothermal treatment at 373 K for 7 days [45]. The silica and titanium sources, tetraethoxysilane (TEOS, 98% purity, Aldrich) and the tetraethyl orthotitanate (TEOT, 80% in water, Aldrich), are used as purchased. Tetrapropylammonium hydroxide (TPAOH, 20% in water, Fluka) is used as structure directing agent (SDA) for the preparation of the MFI type molecular sieve (TS-1 titanosilicate). The silica and titanium sources (TEOS and TEOT) were mixed and stirred for 15 min at RT. In order to avoid the formation of dense TiO_2 phases, the aqueous solution of TPAOH was introduced drop wise to the mixture, and then the suspension was stirred for 1 h at RT. After the synthesis, the crystalline suspension was purified by high speed centrifugation and subsequently redispersed in water. The milky colloidal suspension of TS-1 with a solid concentration of 4 wt.% was deposited on watch glass and polypropylene UV cell. The drying process was performed at 341 K overnight (evaporation rate of 0.02 mL h^{-1}). Humidity and temperature were measured by hygrothermometer during the evaporation of the water from the colloidal suspension. The stability of the TS-1 hierarchical structure after calcination (573 K) and on self-assembled tablets (prior IR characterization) is verified by scanning electron microscopy (SEM). The macropores in the samples are preserved as shown by the SEM pictures. Additionally, the mercury intrusion analysis proved the preservation of the macropores in the TS-1 hierarchical samples (see the section below).

2.2. Characterization

The materials were characterized by X-ray diffraction (XRD) using a STOE STADI-P diffractometer equipped with a curved germanium (1 1 1) primary monochromator and a linear position-sensitive detector with CuKα1 radiation. The morphology and the regular macroporous structures of the TS-1 materials were imaged by a Philips XL30 scanning electron microscope (SEM). Additionally, transmission electron microscope (TEM) FEI 300 operated at 300 kV is used to characterize the size and crystalline structure of the individual TS-1 nanocrystals.

The size of the crystalline TS-1 particles in the colloidal suspensions prior to the formation of the hierarchical structures was determined by dynamic light scattering (DLS) using a Malvern Zetasizer-Nano instrument.

The presence of titanium in the TS-1 sample was confirmed by recording the UV–vis spectra from colloidal suspensions using a Hewlett Packard HP8453 spectrometer, and EDX–SEM study on powder samples was carried out as well.

Nitrogen sorption isotherms at 77 K were collected on a Micromeritics ASAP micropore analyser (samples were degassed at 573 K for 24 h). The mercury intrusion analysis was performed on AutoPoreIII 9410® porosimeter from Micromeritics. The maximum working pressure was 330 MPa, which covers the pores with diameters ranging from about 220 μm to 3 nm. The volume of mercury injected in the sample is determined by measuring the electrical capacity of the sample carrier.

2.3. Adsorption of probe molecules in TS-1 hierarchical structures

Prior adsorption of the probe molecules, the hierarchical TS-1 material in the form of a wafer of 2 cm^2 surface (10 mg, 5 mg cm^{-2}) was treated by cold plasma (air gas mixture at low pressure of 5 hPa). The removal of the TPA from the TS-1 hierarchical structure at room temperature was followed by FTIR. The dielectric barrier discharge was ignited with a 50 Hz sinusoidal power supply (2 kV) between two electrodes fused to the IR cell. The temperature increase due to the cold plasma process was below ΔT = 20 K. The IR spectra were collected in transmission mode on a Bruker vertex 80v equipped with a cryogenic MCT detector (4 cm^{-1} resolution, 8 scans, 1.2 s acquisition time).

The interaction of 2,4,6-trimethylpyridine (collidine) in the TS-1 macrostructures has been followed by FTIR. Before introducing the probe, the sample was activated at 423 K for 30 min in order to remove the residual water sorbed during the transfer of the sample from the plasma reactor to the IR cell. After acquisition of the spectra of the activated material, collidine was introduced. The spectrum for collidine on the TS-1 samples was collected after contacting time of 10 min under a pressure of 3 hPa. Then, a second spectrum was recorded after pumping for 30 min at room temperature.

3. Results and discussion

3.1. Physicochemical characterization of TS-1 structures

The crystalline structure of the sample is confirmed by XRD analysis (Fig. 1a). The X-ray pattern shows that the sample consists of a highly crystalline TS-1 zeolite with MFI-type structure. Only the Bragg peaks corresponding to the MFI-type zeolite (see X-ray pattern of silicalite-1) are present and no signatures for any other crystalline phase or amorphous materials are observed. The broadening of the Bragg peaks is attributed to the nanosized TS-1

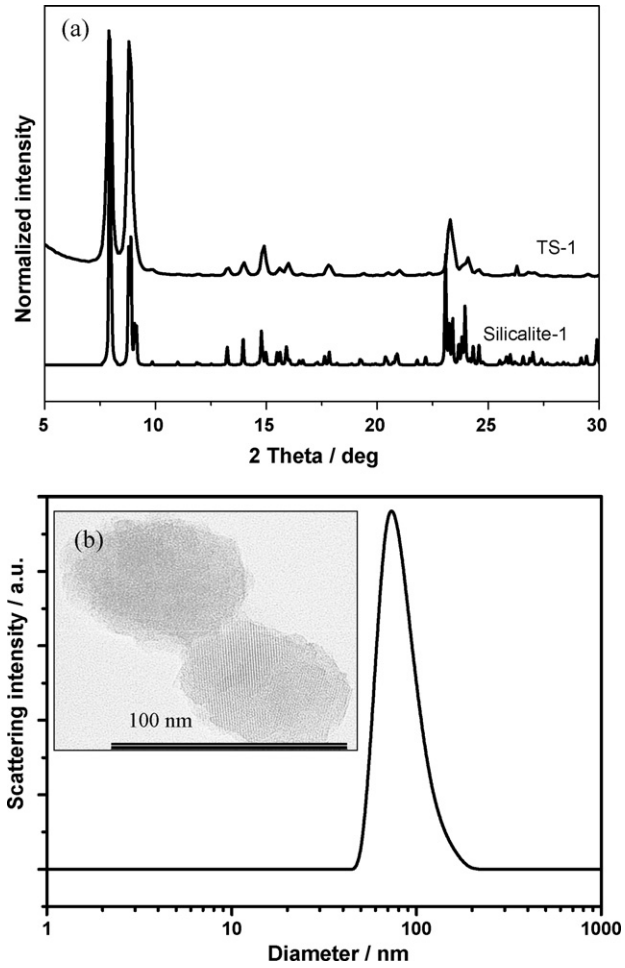

Fig. 1. (a) X-ray patterns of TS-1 and silicalite-1 powder samples, and (b) dynamic light scattering (DLS) curve of TS-1. *Insert*: TEM micrograph of the TS-1 nanocrystals.

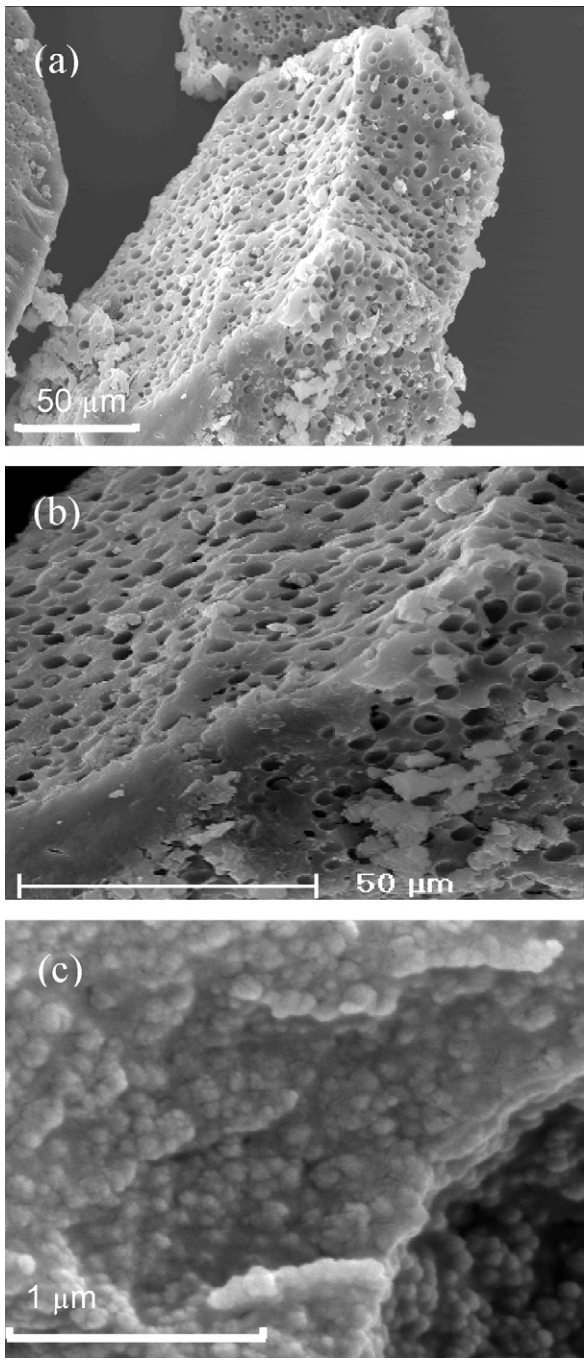

Fig. 2. SEM micrographs of (a and b) TS-1 hierarchical bulk structures, and (c) walls of the macropores consisting of densely packed TS-1 nanocrystals.

crystals. Besides, the particle size, morphology and crystallinity of the TS-1 nanocrystals are proven by TEM study (insert of Fig. 1b). As can be seen, the TS-1 nanoparticles are fully crystalline and the lattice fringes characteristic for the MFI type structure can be seen well aligned within the single TS-1 crystals. The nanosized crystals have almost spheroidal shape and the average crystal size is around 60–80 nm.

In addition to the TEM characterization, the particle size distribution (PSD) in the TS-1 suspensions prior to evaporation of water and assembling into hierarchical porous structures is determined at a constant pH = 12 and a concentration of solid particles of 4 wt.% by DLS. As can be seen from the DLS curve in Fig. 1b, the suspension contains particles with monomodal PSD, and a single peak at 70 nm is present. A dynamic aggregation may occur in the TS-1 suspension that explains the rather broad particle size distribution curve.

The Ti loading in the TS-1 nanocrystals is 1.8 wt.% as determined by chemical analysis. Supplementary elemental cartography measurements on the TS-1 sample by EDX–SEM are carried out. The maps for Si and Ti in an area of 100 μm^2 covered with TS-1 nanocrystals showed that the titanium distribution is very homogeneous within the crystals (supporting information, S1). Additionally, the UV–vis spectrum of the TS-1 colloidal suspension is recorded. The spectrum displays two absorption bands at 210 and 250 nm (supporting information, S2). The first absorption band at 210 nm is assigned to the electron excitation from ligand oxygen to an unoccupied orbital of the framework Ti^{4+} ($p\pi$–$d\pi$ charge transfer transition), while the band at 250 nm could be attributed to some extra framework titanium species. No bands assigned to TiO_2 anatase like oxide phases at about 300 nm or above are observed [46,47].

The TS-1 hierarchical structure is formed by controlled evaporation of the colloidal suspension deposited on watch glass (0.02 mL h^{-1} evaporation rate). The SEM pictures (Fig. 2) reveal the presence of compact three dimensional structures (bodies) with a thickness of about 50 μm (Fig. 2a). The surface of these structural bodies contains uniform holes which are the apertures of macropores with a size of 1–5 μm. The aperture of the macropores appears with almost spherical shape (Fig. 2b), and no cylinders deeply penetrating in the three dimensional structures can be distinguished in the SEM pictures. However, it is important to note that entire TS-1

bulk material has the same appearance. The walls of the macropores are composed of densely packed nanosized TS-1 crystals (Fig. 2c).

Series of evaporation experiments using the same TS-1 colloidal suspension on watch glass of 100 mm diameter and disposable polypropylene UV cell (12.5 mm × 12.5 mm × 45 mm) are performed. Only the TS-1 nanocrystals dried on the watch glass possess the hierarchical features after water evaporation. The convective flow mechanism of water evaporation together with the surface of the watch glass could explain the formation of such organized hierarchical structures. Indeed, the solvent evaporation on the watch glass produces motion of colloidal particles against the meniscus (convective flows which can be considerable on the nanometer length scale). The nanosized TS-1 particles present in the colloidal suspension are carried by the solvent convective flow to their final destination. The electrostatic repulsion and Van der Waals attraction between the nanosized TS-1 particles could then stabilize and preserve the assemblies formed. Indeed, the relatively weak attractions between nanocrystals, which are efficiently screened in solution, become considerable as the solvent is evaporated and stabilize the evolving hierarchical structure. It should be noted that the self assembly behaviour of the TS-1 nanosized crystals is not observed in silicalite-1 suspensions subjected to the same evaporation procedure (see supporting information, S3).

The hierarchical TS-1 structure is confirmed by recording the nitrogen sorption isotherm (Fig. 3) and the mercury intrusion (Fig. 4). At low relative pressure ($P/P^o < 0.1$) the sorption of nitrogen in the micropores is evidenced by a steep uptake. Besides, the hysteresis loop at about $P/P^o = 0.9$ confirms the presence of mesopores. After its upper closure at $P/P^o = 0.95$, an additional sorption of nitrogen occurs at the surface or in the volume of the macropores. The total pore volume vague calculated at $P/P^o = 0.99$ is about 0.42 $cm^3\,g^{-1}$. The pore size distribution determined from the adsorption branch using the BJH method is shown as insert in Fig. 3a. A mono-modal distribution of mesopores centered at 10 nm is apparent. Surface areas and pore volumes for the TS-1 hierarchical sample are determined by the alpha-plot method using Silica-1000 (22.1 $m^2\,g^{-1}$) as a reference (Table 1). The microporous volume, $V_{micro} = 0.13\ cm^3\,g^{-1}$ is typical for TS-1 material, which confirms the purity of the crystalline phase. The porosity of the sample is also investigated by mercury porosimetry (Fig. 4). The pore diameter is estimated in the whole pressure range using the Washburn equation, i.e. $d = -4\gamma\cos\varphi/P$, where d is the diameter of pores (m), P the applied pressure (Pa), γ the superficial tension of the mercury (0.48 $N\,m^{-1}$) and φ the contact angle (130°) [48]. Three regions in the intrusion curve can be clearly distinguished. The greatest part of the intrusion volume (0.66 $cm^3\,g^{-1}$) is taken under 0.12 MPa pressure, which is assigned to mercury intrusion in the very wide macropores ($d > 10\ \mu m$) that are interstitial between the three-dimensional TS-1 bodies. A second uptake (0.17 $cm^3\,g^{-1}$) is seen above the pressure of 25 MPa, which corresponds to the filling of mesopores ($d < 0.05\ \mu m$) of the TS-1 hierarchical material. The flat uptake ($V_{macro} = 0.06\ cm^3\,g^{-1}$) is from the intrusion of mercury in the macropores built in the three dimensional TS-1 bodies as shown in the SEM pictures (Fig. 2). This value is lower but close to the one estimated from the upper part of the N_2 isotherm (0.12 $cm^3\,g^{-1}$). The macroporosity in the TS-1 hierarchical bodies is about 15–30% from the total porosity. The surface covered by the apertures of these macropores is roughly estimated to be about 25% based on the SEM (see Fig. 2). If the macropores are cylindrical and running across the TS-1 macrostructure, this would infer a ratio of macropores volume/pores volume roughly equal to ¼. This estimation is in favor of cylindrical macropores deeply penetrating in the three dimensional TS-1 bodies. A schematic presentation of the hierarchical porosity of the TS-1 material is given in Fig. 5. The TS-1 hierarchical structure contains a regular microporosity coming from the crystalline TS-1, a narrow distribution of mesopores with

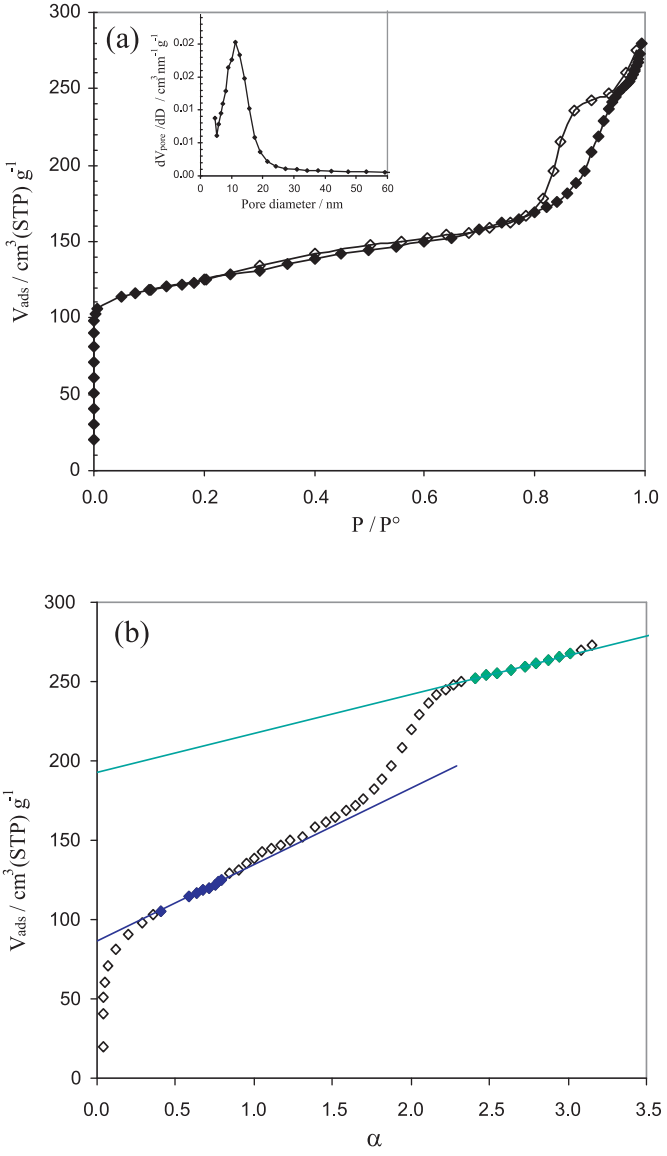

Fig. 3. TS-1 hierarchical structure: (a) N_2 sorption isotherm (full symbols correspond to adsorption and open symbols correspond to desorption branches). *Insert*: pore size distribution; (b) alpha-plot presentation of N_2 sorption isotherm.

size of 10 nm due to the packing of the spheroidal nanocrystals with a constant size, and macroporosity emerging from the bubbled convective evaporation of water. Besides, extra-large macropores due to packing of the macrostructured three dimensional TS-1 bodies are created.

3.2. Adsorption of probe molecule in TS-1 hierarchical structures

The TS-1 hierarchical material was treated by plasma under air gas mixture prior adsorption of probe molecule. As shown in Fig. 6, an almost complete elimination of the organic template (TPA) from the hierarchical TS-1 sample is observed. The IR bands in the range of 3000–2900 cm^{-1} due to the νCH stretching (fingerprint of the organic template) decrease very fast. About 80% of TPA is removed from the TS-1 structure during the first second, then the reaction rate of the template removal decreases (insert in Fig. 6). Since the electrical discharge has preferential direction in the solid material, a part of the wafer is not treated and about 8% of the template is retained in the TS-1 hierarchical structure after 60 s treatment. The band of molecular adsorbed water (*ca.* 1630 cm^{-1}, δ_{H_2O}) dis-

Table 1
Textural properties of TS-1 hierarchical material.

Sample	S_{meso} ($m^2\ g^{-1}$)	S_{macro} ($m^2\ g^{-1}$)	V_{micro} ($cm^3\ g^{-1}$)	V_{meso} ($cm^3\ g^{-1}$)	V_{macro} ($cm^3\ g^{-1}$)	$V_{wide\ macro}$ ($cm^3\ g^{-1}$)
TS-1[a]	57	60	0.13	0.16	0.12	–
TS-1[b]	–	–	–	0.17	0.06	0.66

[a] Based on nitrogen sorption experiment.
[b] Based on mercury intrusion porosimetry.

appears in the first 2 spectra and the νOH band of Si–OH groups at 3740 cm^{-1} are appeared. The very fast removal of the organic template is mainly due to the presence of superficial water on the TS-1 material since the Ti–O generates hydrophilic regions. After the plasma ignition, the water molecules become a source of active species (radicals) which participates in the template elimination [44].

The template-free TS-1 hierarchical structures are exposed to collidine, which has a kinetic diameter of 0.74 nm. The TS-1 nanocrystals consist of straight channels (0.51 nm × 0.55 nm) intersected by zig–zag channels (0.53 nm × 0.56 nm). Theoretically, the bulky collidine probe cannot penetrate into the micropores of TS-1 zeolite. Consequently, its adsorption enables to probe interaction with adsorption sites located in meso- and macro-pores. The IR spectra of the TS-1 sample under adsorption and desorption of collidine in the region of 4000–1500 cm^{-1} are presented in Fig. 7. The first spectrum (Fig. 7a) is recorded under 3 hPa pressure of collidine,

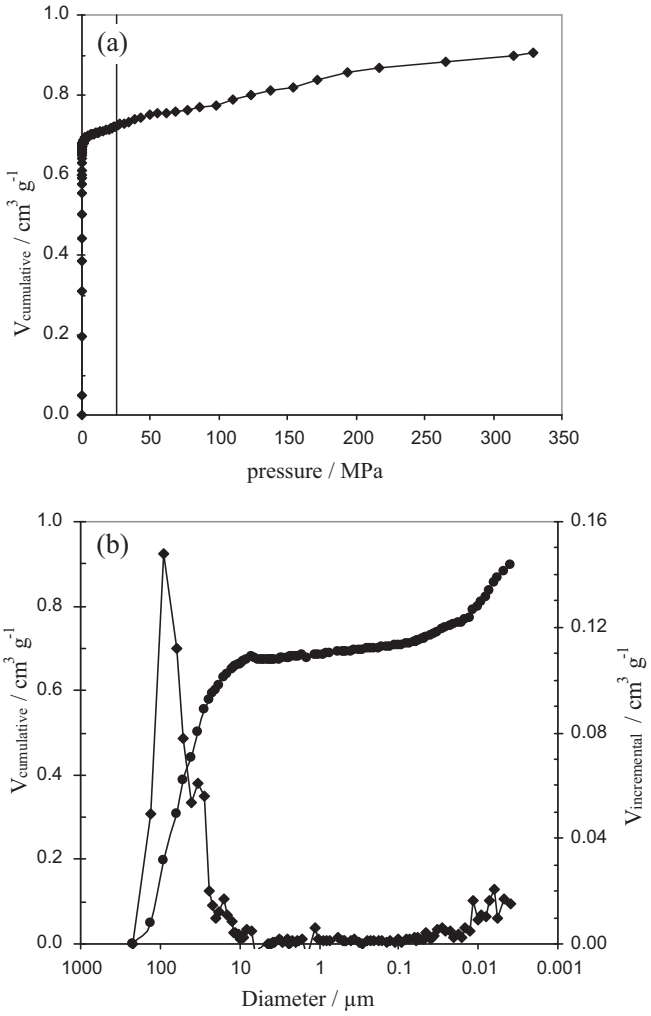

Fig. 4. (a) Mercury intrusion curve of TS-1 hierarchical structure and (b) pore size distribution determined from Hg porosimetry.

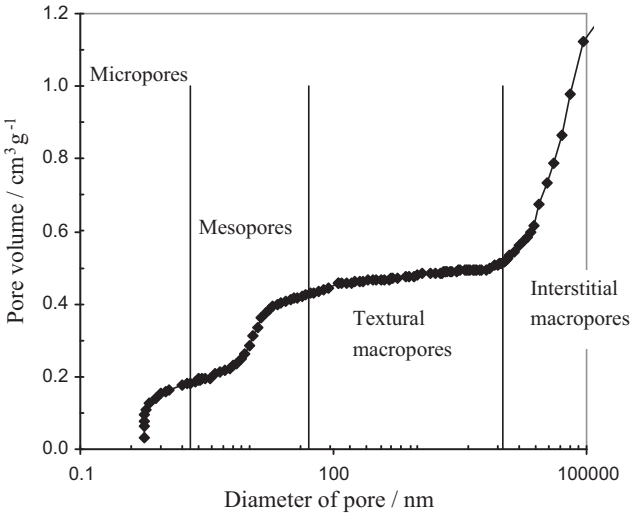

Fig. 5. Schematic representation of hierarchical porosity of TS-1 material: (i) micropore size distribution is determined from the N_2 isotherm using Saito–Folley analysis method, (ii) mesopore size distribution is determined from the N_2 adsorption branch using the BJH analysis, and (iii) macropore size distribution is determined from the Hg porosimetry using Washburn equation.

while the second spectrum (Fig. 7b) is collected after evacuation (desorption) at RT for 10 min. In addition the spectrum of collidine in dilute solution of CCl_4 is shown in Fig. 7c (NIST data-base). The spectrum of collidine adsorbed on the TS-1 displays the νCH bands and two breathing vibrations of aromatic cycle at 1613 cm^{-1} and 1570 cm^{-1}, which are present in the spectrum of collidine in CCl_4. The silanol band is strongly affected (about 50%) and no signal arising from perturbed νOH is seen (a broad band is overlapping with the νCH). However, two small bands at 1650 cm^{-1} (sh) and 1637 cm^{-1} reveal the presence of collidinium species and indicate

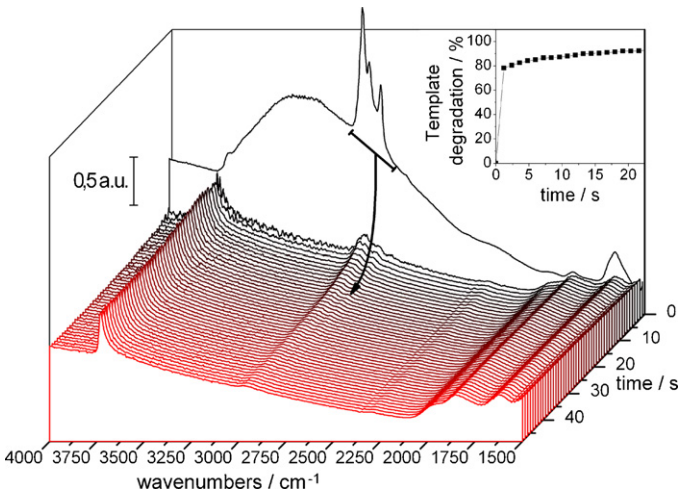

Fig. 6. FTIR spectra of TS-1 hierarchical structure under non-thermal plasma treatment in an air gas mixture (5 hPa). *Insert*: removal of the template (TPA) from the TS-1 material with time.

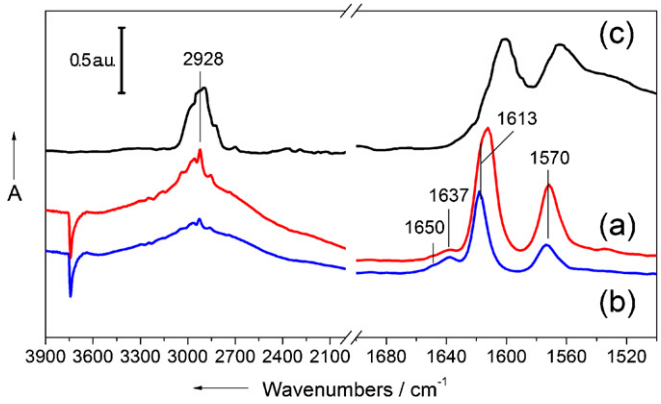

Fig. 7. FTIR spectra of TS-1 hierarchical structure at RT contacting with collidine (a) after 10 min under pressure of 3 hPa and (b) after 30 min desorption. The IR spectrum of collidine dilute in CCl_4 is reported in (c).

that a part of the acidic Brønsted sites are interacting with the alkylpyridine probe [49]. Although no band from acidic (Si,Ti)–OH species is recorded in the IR spectrum of the TS-1 material, some Brønsted acidic sites able to protonate the collidine base are present outside the micropores. In conclusion, the hierarchical porous network seems to slightly improve the accessibility of the acid sites present in the TS-1 structure. In the present case, the probe adsorption experiments were performed at RT, probe diffusion and further interactions on the solid are expected to be enhanced at higher temperature. The accessibility index (ACI) of such TS-1 hierarchical material will be investigated in details in future works.

4. Conclusions

Tailoring of hierarchical structures by controlled water evaporation of colloidal suspension containing TS-1 nanocrystals is demonstrated. The presence of Ti in the porous hierarchical material is proven by UV–vis, EDX–SEM and chemical analysis. The TS-1 hierarchical structures possess uniform micropores, textural mesopores and macropores emerging from the controlled evaporation of the water, confirmed by N_2 sorption and mercury porosimetry. The main driving force for the formation of the hierarchical features in the TS-1 structure is the convective flow of the solvent (water) during the controlled evaporation process. The shape of the meniscus of the suspension appears to have a crucial role on the formation of the hierarchical TS-1 structures.

The hierarchical TS-1 material activated by non-thermal plasma is studied by adsorption/desorption of collidine molecule. Such molecule exhibits a kinetic diameter bigger than the pore opening of TS-1 and is expected to only probe the outer surface and the macroporosity of the hierarchical material. But the formation of collidinium species may indicate that acid sites are also interacting with the collidine. The diffusion/penetration and confinement of the bulky molecule in the hierarchical TS-1 material seem to be improved.

Acknowledgements

The authors gratefully acknowledge funding from the SRIF PNANO ANR Project and CCJensen.

Appendix A. Supplementary data

Supplementary data associated with this article can be found, in the online version, at doi:10.1016/j.cattod.2010.12.045.

References

[1] M. Davis, Nature 417 (2002) 813.
[2] F. Caruso, Chem. Eur. J. 6 (2000) 413.
[3] W. Zhao, H. Chen, Y. Li, L. Li, M. Li, J. Shi, Adv. Funct. Mater. 18 (2008) 2780.
[4] Y. Yin, R.M. Rioux, C.K. Erdonmez, S. Hughes, G.A. Somorjai, A. Alivisatos, Science 304 (2004) 711.
[5] Y. Tao, H. Kanoh, L. Abrams, K. Kaneko, Chem. Rev. 106 (2006) 896.
[6] V. Valtchev, S. Mintova, Micropor. Mesopor. Mater. 43 (2001) 41.
[7] V. Valtchev, Chem. Mater. 14 (2002) 956.
[8] N. Petkov, M. Holzl, T.H. Metzger, S. Mintova, T. Bein, J. Phys. Chem. B 109 (2005) 4485.
[9] J.L.H. Chau, K.L. Yeung, Chem. Commun. 9 (2002) 960.
[10] A. Corma, M. Diaz-Cabanas, J. Martinez-Triguero, F. Rey, J. Rius, Nature 418 (2002) 514.
[11] S. Donk, A.H. Janssen, J.H. Bitter, K.P. Jong, Catal. Rev. 45 (2003) 297.
[12] D. Walsh, A. Kulak, K. Aoki, T. Ikoma, J. Tanaka, S. Mann, Angew. Chem. Int. Ed. 43 (2004) 6691.
[13] S.P.B. Kremer, Ch.E.A. Kirschhock, A. Aerts, K. Villani, J.A. Martens, O.I. Lebedev, G.V. Tendeloo, Adv. Mater. 15 (20) (2003) 1705.
[14] N. Chu, J. Wang, Y. Zhang, J. Yang, J. Lu, D. Yin, Chem. Mater. 22 (2010) 2757.
[15] L. Huang, Z. Wang, J. Sun, L. Miao, Q. Li, Y. Yan, D. Zhao, J. Am. Chem. Soc. 122 (2000) 3530.
[16] X.D. Wang, W.L. Yang, Y. Tang, Y.J. Wang, S.K. Fu, Z. Gao, Chem. Commun. 21 (2000) 2161.
[17] A. Dong, Y. Wang, Y. Tang, N. Ren, Y. Zhang, Z. Gao, Chem. Mater. 14 (2002) 3217.
[18] A. Dong, N. Ren, W. Yang, Y. Wang, Y. Zhang, D. Wang, J. Hu, Z. Gao, Y. Tang, Adv. Funct. Mater. 13 (12) (2003) 943.
[19] V. Valtchev, Chem. Mater. 14 (2002) 4371.
[20] B. Zhang, S.A. Davis, N.H. Mendelson, S. Mann, Chem. Commun. 9 (2000) 781.
[21] B. Zhang, S.A. Davis, S. Mann, Chem. Mater. 14 (2002) 1369.
[22] Y.J. Lee, J.S. Lee, Y.S. Park, K.B. Yoon, Adv. Mater. 13 (2001) 95.
[23] K. Zhu, D. Wang, J. Liu, Nano Res. 2 (2009) 129.
[24] K.T. Jung, J.H. Hyun, Y.G. Shul, Zeolites 19 (1997) 161.
[25] O. Ugursoy, S. Vahdettin, Powder Technol. 183 (2008) 207.
[26] B. Notari, Adv. Catal. 41 (1996) 253.
[27] Y. Hasegawa, A. Ayame, Catal. Today 71 (2001) 177.
[28] N. Bruno, 235th ACS Meeting, New Orleans, LA, USA, April 6–10, American Chemical Society, Washington, DC, 2008, IEC-125, CODEN: 69KNN3.
[29] D. Serrano, R. Sanz, P. Pizarro, I. Moreno, Chem. Commun. 11 (2009) 1407.
[30] M. Reichinger, W. Schmidt, M.W.E. van den Berg, A. Aerts, J.A. Martens, Ch.E.A. Kirschhock, H. Gies, W. Grünert, J. Catal. 269 (2010) 367.
[31] S. Tsai, P. Chao, T. Tsai, I. Wang, X. Liu, X. Guo, Catal. Today 148 (2009) 174.
[32] H. Xin, J. Zhao, S. Xu, J. Li, W. Zhang, X. Guo, E.J.M. Hensen, Q. Yang, C. Li, J. Phys. Chem. C 114 (2010) 6553.
[33] X. Zhang, Y. Wang, F. Xin, Appl. Catal. A: Gen. 307 (2006) 222.
[34] Y.S.S. Wan, A. Gavriilidis, K.L. Yeung, React. Eng. Microstruct. React. 81 (August) (2003) 753.
[35] H. Munakata, Y. Oumi, A. Miyamoto, Phys. Chem. B 105 (2001) 3493.
[36] T. Atoguchi, S. Yao, J. Mol. Catal. A: Chem. 176 (2001) 173.
[37] G.B. Shul'pin, T. Sooknoi, V.B. Romakh, G. Süss-Fink, L.S. Shul'pina, Tetrahedron Lett. 47 (2006) 3071.
[38] I. Schmidt, A. Krogh, K. Wienberg, A. Carlsson, M. Brorson, C.J.H. Jacobsen, Chem. Commun. 21 (2000) 2157.
[39] Y. Fang, H. Hu, Catal. Commun. 8 (5) (2007) 817.
[40] X. Ke, L. Xu, C. Zeng, L. Zhang, N. Xu, Micropor. Mesopor. Mater. 106 (2007) 68.
[41] Y. Cheneviere, F. Chieux, V. Caps, A. Tuel, J. Catal. 269 (2010) 161.
[42] D.P. Serrano, R. Sanz, P. Pizarro, I. Moreno, Top Catal. 53 (2010) 1319.
[43] J. Patarin, Angew. Chem. Int. Ed. 43 (2004) 3878.
[44] M. Rivallan, I. Yordanov, S. Thomas, C. Lancelot, S. Mintova, F. Thibault-Starzyk, ChemCatChem 2 (2010) 1074.
[45] G. Zhang, J. Sterte, B.J. Schoeman, Chem. Mater. 9 (1997) 210.
[46] J.A. Creighton, D.G. Eadon, J. Chem. Soc., Faraday Trans. 87 (1991) 3881.
[47] Y. Ding, Q. Gao, B. Wang, G. Li, L. Yan, J. Porous Mater. 12 (2005) 131.
[48] Y.S. Ko, W.S. Ahn, Korean J. Chem. Eng. 15 (1998) 182.
[49] F. Thibault-Starzyk, A. Vimont, J.-P. Gilson, Catal. Today 70 (2001) 227.